

# SCIENTIFIC REPORTS



OPEN

## A highly selective and sensitive near-infrared fluorescent probe for imaging of hydrogen sulphide in living cells and mice

Received: 01 September 2015

Accepted: 30 November 2015

Published: 08 January 2016

Ling Zhang<sup>1,2,\*</sup>, Xi Emily Zheng<sup>4,\*</sup>, Fang Zou<sup>2</sup>, Yanguo Shang<sup>2</sup>, Wenqi Meng<sup>2</sup>, En Lai<sup>1</sup>, Zhichen Xu<sup>1</sup>, Yi Liu<sup>2</sup> & Jing Zhao<sup>1,3</sup>

Hydrogen sulphide (H<sub>2</sub>S), the third endogenous gaseous signalling molecule, has attracted attention in biochemical research. The selective detection of H<sub>2</sub>S in living systems is essential for studying its functions. Fluorescence detection methods have become useful tools to explore the physiological roles of H<sub>2</sub>S because of their real-time and non-destructive characteristics. Herein we report a near-infrared fluorescent probe, NIR-HS, capable of tracking H<sub>2</sub>S in living organisms. With high sensitivity, good selectivity and low cytotoxicity, NIR-HS was able to recognize both the exogenous and endogenous H<sub>2</sub>S in living cells. More importantly, it realized the visualization of endogenous H<sub>2</sub>S generated in cells overexpressing cystathionine β-synthase (CBS), one of the enzymes responsible for producing endogenous H<sub>2</sub>S. The probe was also successfully applied to detect both the exogenous and endogenous H<sub>2</sub>S in living mice. The superior sensing properties of the probe render it a valuable research tool in the H<sub>2</sub>S-related medical research.

Hydrogen sulphide (H<sub>2</sub>S) has emerged as the third endogenous gaseous signalling molecule in living organisms, along with nitric oxide (NO) and carbon monoxide (CO)<sup>1,2</sup>. It is mainly produced by enzymes such as cystathionine β-synthetase (CBS), cystathionine γ-lyase (CSE) and cysteine aminotransferase (CAT)/3-mercaptopyruvate sulphurtransferase (3-MST)<sup>3</sup>. Physiological levels of H<sub>2</sub>S have diverse biological functions, including neurotransmission<sup>4</sup>, vasodilation<sup>5</sup>, apoptosis<sup>6</sup>, inflammation<sup>7</sup>, ischemia/reperfusion-induced injury<sup>8</sup> and insulin secretion<sup>9</sup>. In addition, abnormal concentrations of H<sub>2</sub>S appear to be involved in many diseases<sup>10,11</sup>, such as Alzheimer's disease and diabetes mellitus.

With increasing interest in understanding the chemical and biological properties of H<sub>2</sub>S, sensitive and selective detection techniques for monitoring endogenous H<sub>2</sub>S are urgently desirable, since the complex manifestations of H<sub>2</sub>S in both physiological and pathological states, as well as its underlying molecular events are still not fully understood. The current approaches for H<sub>2</sub>S detection, such as the methylene blue method, the monobromobimane (MBB) method, gas chromatography (GC), and the sulphide ion selective electrodes (ISE) method are not suitable for *in situ* analysis<sup>12</sup>. Fluorescence-based assays, however, could offer convenience, high sensitivity, nondestructiveness, as well as real-time imaging<sup>13</sup>.

Recently, various sensing strategies have been focused on the design of H<sub>2</sub>S-reactive probes, including nucleophilic addition<sup>14–20</sup>, copper sulphide precipitation<sup>21–23</sup>, H<sub>2</sub>S-mediated reduction<sup>24–29</sup>, and the thiolysis of dinitrophenyl ether by H<sub>2</sub>S<sup>30,31</sup>, *etc.*<sup>32</sup>. However, most of these fluorescent probes are based on fluorophores with peaks in the ultraviolet-visible (UV/V is) region, which renders them difficult to be employed for imaging H<sub>2</sub>S in living animals due to high absorption and autofluorescence of biomolecules<sup>33</sup>. By contrast, probes with absorption and emission in the near-infrared (NIR) region are more desirable for *in vivo* imaging because of minimal photo damage, deep

<sup>1</sup>School of Chemistry and Chemical Engineering, Nanjing University, Nanjing, 210093, China. <sup>2</sup>Jiangsu Key Laboratory of New Drug Research and Clinical Pharmacy, School of Pharmacy, Xuzhou Medical College, Xuzhou, 221002, China.

<sup>3</sup>Guangdong Key Lab of Nano-Micro Material Research, School of Chemical Biology and Biotechnology, Peking University Shenzhen Graduate School, Shenzhen, 518055, China. <sup>4</sup>Department of Gastroenterology, Nanjing Drum Tower Hospital, The Affiliated Hospital of Nanjing University Medical School, Nanjing, 210029, China. \*These authors contributed equally to this work.

Correspondence and requests for materials should be addressed to L.Z. (email: zhangling1999@163.com) or Y. L. (email: njliuyi@163.com) or J.Z. (email: jingzhao@nju.edu.cn)

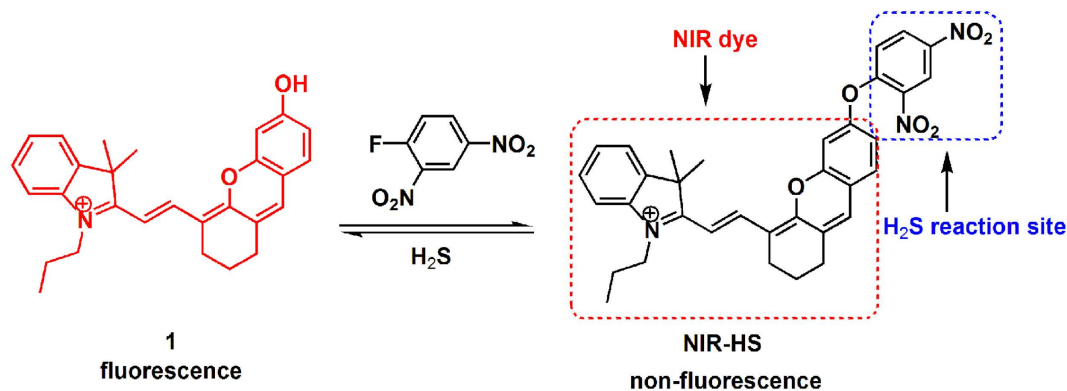


**Figure 1.** Design and synthesis of NIR fluorescent turn-on probe NIR-HS.

tissue penetration, and minimum interference from background autofluorescence<sup>34</sup>. Recently, several research groups have reported excellent NIR fluorescent probes for H<sub>2</sub>S<sup>35–43</sup>. Lin *et al.* prepared a NIR fluorescent probe by utilizing thiolysis of dinitrophenyl ether<sup>38</sup>. Tang *et al.* constructed a NIR ratiometric fluorescent probe for rapid imaging of endogenous H<sub>2</sub>S *via* nucleophilic addition with an impressive detection limit of 5.0–10.0 nM<sup>40</sup>. Guo *et al.* introduced a NIR fluorescent probe based on selective complexation ability with copper<sup>41</sup>. Despite these progresses, we are interested in developing practical NIR probes with a combination of desirable characteristics, especially low detection limits and the ability to detect endogenous H<sub>2</sub>S in living animals. Fluorescent probes with a lower detection limit, especially the nanomole range, or even lower, are needed owing to the low levels of endogenous H<sub>2</sub>S in cells/plasma/tissues. Moreover, the probes for detection of endogenous H<sub>2</sub>S *in vivo* are still sparse<sup>44,45</sup>. Thus, NIR probes with higher sensitivity and favourable properties to monitor endogenous H<sub>2</sub>S *in vivo* are in high demand.

Herein, we prepared NIR-HS as a NIR fluorescent probe for H<sub>2</sub>S detection. The key features of NIR-HS include good selectivity, high sensitivity and suitability for recognizing endogenous H<sub>2</sub>S in living cells and mice.

## Results and Discussion

**Synthesis and sensing mechanism of NIR-HS.** In the design of a NIR probe for H<sub>2</sub>S, the hemicyanine skeleton (a NIR dye) was selected as a fluorophore in the light of its NIR emission and high stability<sup>46</sup>. It is known that the thiolysis of the dinitrophenyl ether reaction can be chemoselective for H<sub>2</sub>S over biothiols<sup>38</sup>. Thus, probe NIR-HS was constructed by connecting a dinitrophenyl group to hemicyanine (a NIR dye) via an ether-linkage (Fig. 1). The fluorescence of NIR-HS was quenched due to alkylation on the hydroxyl group<sup>46</sup>. We speculated that the reaction of sulphide with NIR-HS would cleave an ether group, and release the free fluorophore, thereby achieving fluorescence detection of sulphide. On the basis of this design, the structure of NIR-HS and the proposed sensing mechanism are illustrated in Fig. 1. The probe was readily synthesised in two steps. Treatment of IR-780 with resorcin in the presence of K<sub>2</sub>CO<sub>3</sub> afforded compound 1, which was then condensed with 1-fluoro-2,4-dinitrobenzene to generate target compound NIR-HS (please refer to the Supplementary Information for details). Finally, target probe, NIR-HS, was characterized by NMR spectroscopy and mass spectrometry (please refer to the Supplementary Information for details).

The reaction of NIR-HS with sulphide produced a red fluorescent product, which was identical to the absorption and emission of the authentic compound 1 (Supplementary Fig. S1). Moreover, the thiolysis product was characterised by HRMS and <sup>1</sup>H NMR spectra (please refer to the Supplementary Information for details), demonstrating that the reaction of NIR-HS with sulphide proceeded as designed in Fig. 1.

**Fluorescent properties of NIR-HS.** The fluorescent properties of NIR-HS (10 μM) in the absence and presence of Na<sub>2</sub>S were determined. The free probe was almost nonfluorescent (Fig. 2A). However, treatment of Na<sub>2</sub>S (100 μM) led to a large fluorescence enhancement at 723 nm (50 fold,  $\Phi = 0.13$ ). Figure 2B depicted elevated fluorescence intensities with increasing amounts of Na<sub>2</sub>S (0–300 μM) until a plateau reached at 100 μM Na<sub>2</sub>S. An excellent linear correlation between the observed fluorescence intensities and various concentrations of Na<sub>2</sub>S (0–100 μM) was observed in PBS buffer (Fig. 2B inset). The *in vitro* detection limit for sulphide was 38 nM, which was lower than most of the reported NIR H<sub>2</sub>S probes. Therefore, NIR-HS is highly sensitive to low-nanomolar levels of sulphide, which facilitate the quantitative detection of endogenous/intracellular H<sub>2</sub>S in complex biological systems.

The fluorescence intensity in reaction of NIR-HS with Na<sub>2</sub>S reached the maximum value within approximately 20 min (Supplementary Fig. S2). The effects of pH on the detection of sulphide were then evaluated (Supplementary Fig. S3). In the pH range from 5.8 to 6.0, the emission intensities were quite low and did not change significantly. From pH 6.2 to 6.8, the fluorescence intensities were gradually increased, and the maximal fluorescence intensities were observed from pH 7.0 to 9.0. The emission profile of fluorophore (compound 1) (Supplementary Fig. S4) are consistent with the results of treating the probe with Na<sub>2</sub>S in different pH PBS buffer, indicating that the observed pH profile is due to the fluorophore itself. Taken together, NIR-HS is suitable for the detection of sulphide between pH 7.0 and 9.0.

**Selectivity to sulphide of NIR-HS.** To investigate the selectivity of NIR-HS towards sulphide, NIR-HS was treated with various species. NIR-HS displayed high selectivity for H<sub>2</sub>S over physiological concentrations of

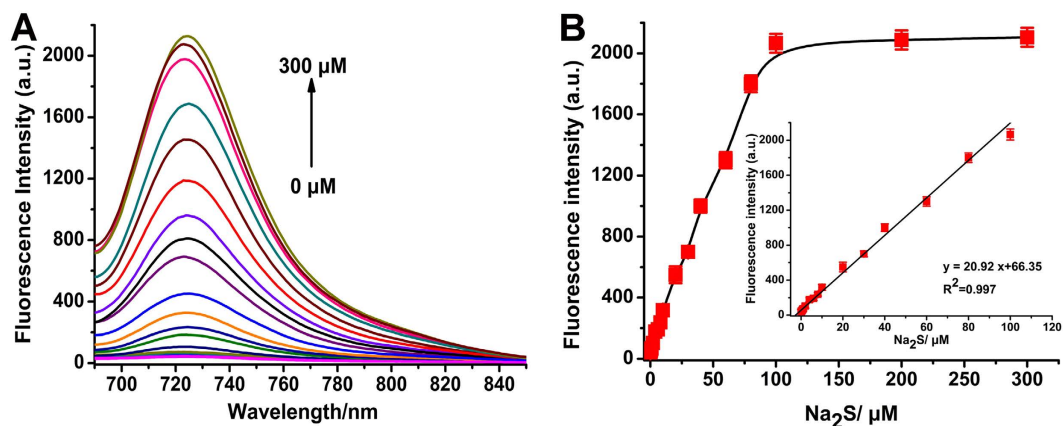


**Figure 2. Fluorescence response of NIR-HS to sulphide.** (A) Fluorescence spectra of NIR-HS (10  $\mu\text{M}$ ) with  $\text{Na}_2\text{S}$  (0, 0.05, 0.1, 0.2, 0.4, 0.6, 0.8, 1, 2, 4, 6, 8, 10, 20, 30, 40, 60, 80, 100, 200 and 300  $\mu\text{M}$ ) in PBS buffer (20 mM, pH = 7.4, 5%  $\text{CH}_3\text{CN}$ ) at 37  $^\circ\text{C}$  for 20 min. (B) The fluorescence intensity changes of NIR-HS (10  $\mu\text{M}$ ) at 723 nm after incubation with different concentrations of  $\text{Na}_2\text{S}$  (0–300  $\mu\text{M}$ ). Inset: The linear relationship between the fluorescence intensity and the concentrations of  $\text{Na}_2\text{S}$  (0 to 100  $\mu\text{M}$ ) in PBS buffer. Data are presented as the mean  $\pm$  SD ( $n = 3$ ).

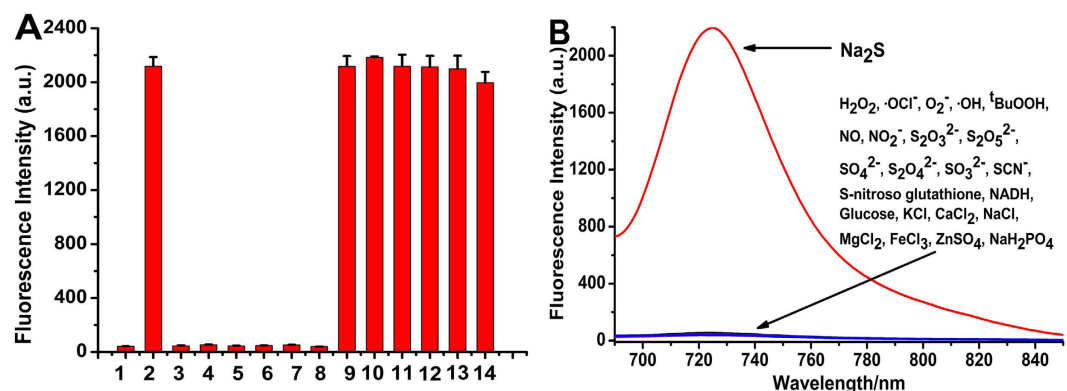


**Figure 3. The selectivity of NIR-HS for sulphide.** (A) Fluorescence responses of NIR-HS (10  $\mu\text{M}$ ) towards  $\text{Na}_2\text{S}$  (100  $\mu\text{M}$ ) and various biothiols after 20 min of incubation. 1.  $\text{Na}_2\text{S}$  (0  $\mu\text{M}$ ); 2.  $\text{Na}_2\text{S}$  (100  $\mu\text{M}$ ); 3. Hcy (100  $\mu\text{M}$ ); 4. GSH (1 mM); 5. Cys (100  $\mu\text{M}$ ); 6. Cys (1 mM); 7. GSH (10 mM); 8. Hcy (1 mM); 9.  $\text{Na}_2\text{S}$  (100  $\mu\text{M}$ ) + Hcy (100  $\mu\text{M}$ ); 10.  $\text{Na}_2\text{S}$  (100  $\mu\text{M}$ ) + Hcy (1 mM); 11.  $\text{Na}_2\text{S}$  (100  $\mu\text{M}$ ) + Cys (100  $\mu\text{M}$ ); 12.  $\text{Na}_2\text{S}$  (100  $\mu\text{M}$ ) + Cys (1 mM); 13.  $\text{Na}_2\text{S}$  (100  $\mu\text{M}$ ) + GSH (1 mM); and 14.  $\text{Na}_2\text{S}$  (100  $\mu\text{M}$ ) + GSH (10 mM). (B) Fluorescence spectra of NIR-HS (10  $\mu\text{M}$ ) towards  $\text{Na}_2\text{S}$  (100  $\mu\text{M}$ ), reactive oxygen species, reactive nitrogen species, sulphur-containing inorganic ions, S-nitroso glutathione (SNG), reducing agents and inorganic salts (1 mM) after 20 min of incubation. Data are presented as the mean  $\pm$  SD ( $n = 3$ ).

biological thiols (Fig. 3A and Supplementary Fig. S5), including glutathione (10 mM GSH), cysteine (1 mM Cys) and homocysteine (1 mM Hcy). The good selectivity of NIR-HS attribute to the stronger nucleophilic properties of  $\text{HS}^-$ , smaller size and a lower pKa at neutral pH compared to other thiols. The remaining non-thiol amino acids (Ala, Glu, Trp, Met, Tyr, Leu, Val, Ser, Pro, Arg, Gly, Phe, His, Gln, Asn, Ile and Thr), reactive oxygen species ( $\text{H}_2\text{O}_2$ ,  $\cdot\text{OCl}^-$ ,  $\text{O}_2^-$ ,  $\cdot\text{OH}$  and  $^t\text{BuOOH}$ ), reactive nitrogen species ( $\text{NO}_2^-$  and NO), sulphur-containing inorganic ions ( $\text{S}_2\text{O}_3^{2-}$ ,  $\text{S}_2\text{O}_5^{2-}$ ,  $\text{SO}_4^{2-}$ ,  $\text{S}_2\text{O}_4^{2-}$ ,  $\text{SO}_3^{2-}$  and  $\text{SCN}^-$ ), S-nitroso glutathione (SNG), reducing agents (NADH and glucose) and inorganic salts (KCl,  $\text{CaCl}_2$ , NaCl,  $\text{MgCl}_2$ ,  $\text{FeCl}_3$ ,  $\text{ZnSO}_4$  and  $\text{NaH}_2\text{PO}_4$ ) induced negligible responses (Fig. 3B and Supplementary Fig. S6). Additionally, competitive experiments also revealed hardly any interference to sulphide detection in the coexistence of  $\text{Na}_2\text{S}$  and various species (Supplementary Fig. S6 and Fig. S7). The fluorescence intensity decreased in the presence of  $\text{H}_2\text{O}_2$  and  $\text{ZnSO}_4$  due to the oxidation of  $\text{H}_2\text{S}$  by  $\text{H}_2\text{O}_2$  and sulphide precipitation of  $\text{H}_2\text{S}$  by  $\text{ZnSO}_4$ . Thus, NIR-HS can be used for the selective detection of sulphide with minimum interference from other biological species.

**Detection of  $\text{H}_2\text{S}$  in living cells.** We thereafter assessed the potential utility of NIR-HS to monitor  $\text{H}_2\text{S}$  in living MCF-7 cells. Prior to cell imaging, MTT assays were performed to evaluate the cytotoxicity of the probe. NIR-HS and compound 1 exhibited  $\text{IC}_{50}$  of  $96.9 \pm 3.2 \mu\text{M}$  and  $99.4 \pm 1.7 \mu\text{M}$ , respectively (Supplementary Figs S8 and S9). These results indicated that cells were variable after incubation with NIR-HS (5  $\mu\text{M}$ ) for 24 h.

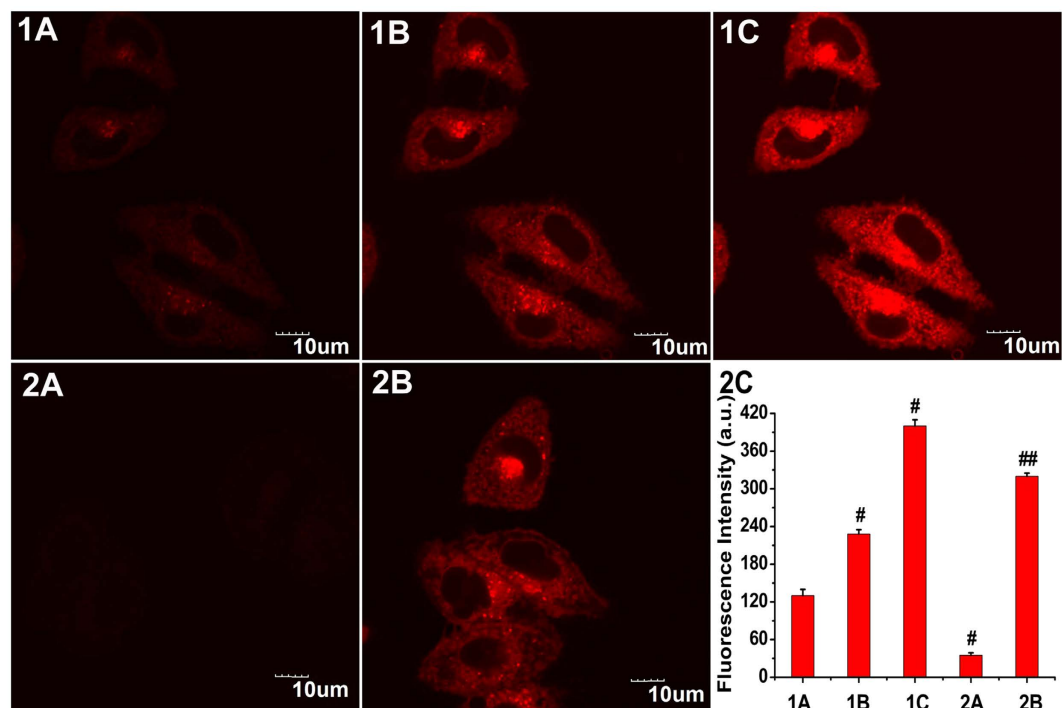


**Figure 4. Confocal fluorescence imaging of exogenous sulphide in living MCF-7 cells using NIR-HS.** Cells were incubated with NIR-HS ( $5\ \mu\text{M}$ ) alone for 10 min (1A). Cells in panel 1A were thereafter treated with  $\text{Na}_2\text{S}$  ( $50\ \mu\text{M}$ ) for 10 min (1B) and 20 min (1C). Cells were pretreated with 1 mM  $\text{ZnCl}_2$  for 10 min, then incubated with NIR-HS ( $5\ \mu\text{M}$ ) for 10 min and  $\text{Na}_2\text{S}$  ( $50\ \mu\text{M}$ ) for 20 min (2A). Cells were incubated with NIR-HS ( $5\ \mu\text{M}$ ) for 10 min and then further incubated with  $\text{Na}_2\text{S}$  ( $25\ \mu\text{M}$ ) for 20 min (2B). Scale bars =  $10\ \mu\text{m}$ . The average fluorescence intensity of the above images (2C). Data are presented as the mean  $\pm$  SD ( $n = 3$ ). # $p < 0.001$  vs. (1A) column, ## $p < 0.001$  vs. (1C) column.

MCF-7 cells incubated with the free probe ( $5\ \mu\text{M}$ ) showed relatively weak fluorescence emission (Fig. 4, panel 1A). In contrast, upon addition of  $\text{Na}_2\text{S}$  ( $50\ \mu\text{M}$ ) to the above cells, a strong red fluorescence was observed (Fig. 4, panel 1B). The sulphide-induced increase of the fluorescence intensity in cells of panel 1B was finished after approximately 20 min (Fig. 4, panel 1C). Subsequently, cells were pretreated with  $\text{ZnCl}_2$  (an efficient eliminator of  $\text{H}_2\text{S}$ ). With the addition of  $\text{Na}_2\text{S}$  ( $50\ \mu\text{M}$ ) to the  $\text{ZnCl}_2$ -pretreated cells, no fluorescence intensity increases were observed (Fig. 4, panel 2A). The results indicated that the fluorescence change of NIR-HS in the cells arises from  $\text{H}_2\text{S}$ . Moreover, the treatment of probe-loaded cells with  $\text{Na}_2\text{S}$  ( $25\ \mu\text{M}$ ) yielded lower fluorescence emission (Fig. 4, panel 2B) compared to the fluorescence of the cells in panel 1C, implying that NIR-HS is capable of imaging different sulphide concentrations in living cells (Fig. 4, panel 2C).

Next, we tested the abilities of NIR-HS to visualize the endogenous  $\text{H}_2\text{S}$ . MCF-7 cells express  $\text{H}_2\text{S}$ -producing enzyme such as CSE<sup>47</sup>. NO could upregulate the CSE expression and stimulate the CSE activity, resulting in increased endogenous  $\text{H}_2\text{S}$  level<sup>48</sup>. Therefore, SNP (Sodium Nitroprusside, a NO donor) was employed to induce the production of endogenous  $\text{H}_2\text{S}$  in MCF-7 cells. The probe-loaded cells exhibited faint fluorescence emission without the addition of SNP (Fig. 5, panel 1A). After incubation of probe-treated cells with SNP (Fig. 5, panel 1B) for another 20 min, the fluorescence signal increased significantly, indicating the generation of endogenous  $\text{H}_2\text{S}$  within the cells. Whereas the cells preincubated with DL-propargylglycine (PPG, an inhibitor for CSE<sup>48</sup>) provided almost no fluorescence enhancement (Fig. 5, panel 1C), demonstrating that the fluorescence change is triggered by endogenously generated  $\text{H}_2\text{S}$ .

CSE and CBS are major enzymes for  $\text{H}_2\text{S}$  production, and the overexpression of CBS or CSE could result in the elevation of endogenous  $\text{H}_2\text{S}$  level<sup>1,2</sup>. We thus constructed the cells with CBS overexpression (Fig. 5, panel 2A). Cells transfected with empty vector (pCMV6) were set as control group (Fig. 5, panel 2B). As shown in Fig. 5, MCF-7 cells that were overexpressing CBS showed much stronger fluorescence (Fig. 5, panel 2A) than that from cells of the control group (Fig. 5, panel 2B), suggesting the increased endogenous level of  $\text{H}_2\text{S}$  in CBS overexpressed cells. The western blot assay proved the overexpression of CBS in cells of panel 2A (Supplementary Fig. S12). We also quantified the fluorescence intensities of these cells, and found that the CBS overexpressed cells showed 2-fold enhanced fluorescence intensity compared to the control cells (Fig. 5, panel 2C). These results revealed the capability of NIR-HS to recognize endogenous  $\text{H}_2\text{S}$  in living cells.

**Detection of  $\text{H}_2\text{S}$  in living mice.** The prominent NIR features of NIR-HS render the probe highly favorable for fluorescence imaging of  $\text{H}_2\text{S}$  in living animals. Inspired by these data, we further examined the suitability of the sensor to visualize exogenous and endogenous  $\text{H}_2\text{S}$  in living mice. Kunming mice were divided into several groups. The mice were given i.p. injection of DMSO as the negative control group (Supplementary Fig. S13, panel

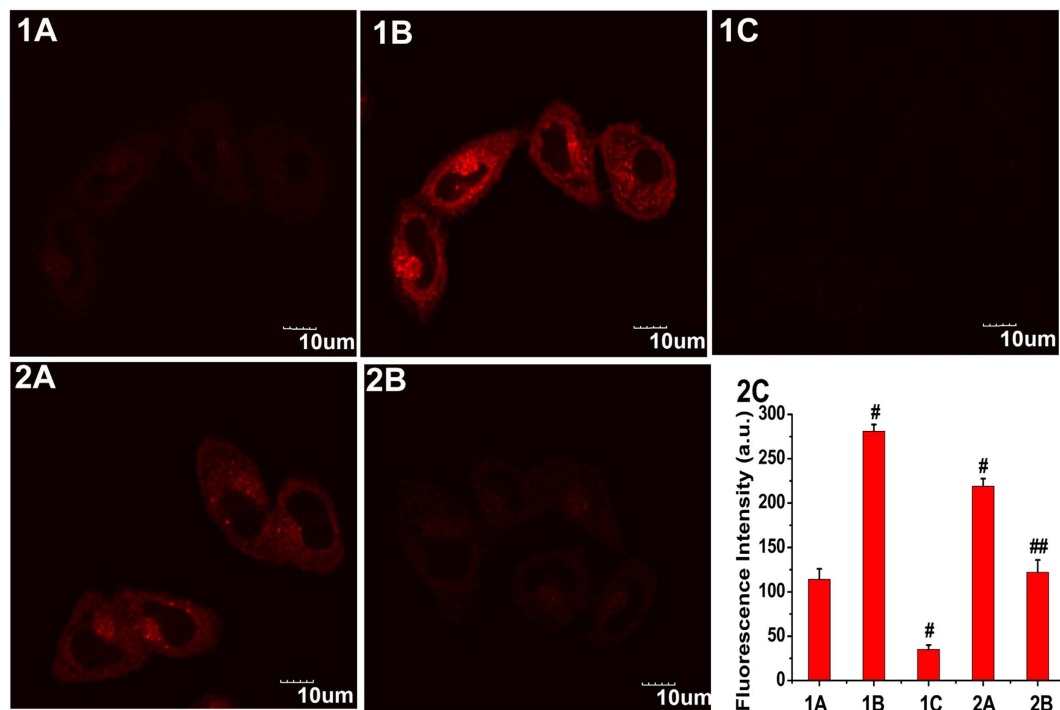


**Figure 5. Confocal fluorescence imaging of endogenous  $H_2S$  in living MCF-7 cells using NIR-HS.** Cells were incubated with NIR-HS ( $5 \mu M$ ) alone for 10 min (**1A**). Cells in panel 1A were thereafter treated with SNP ( $50 \mu M$ ) for 20 min (**1B**). PPG-treated cells were incubated with NIR-HS ( $5 \mu M$ ) for 10 min and then stimulated with SNP ( $50 \mu M$ ) for 20 min (**1C**). Cells with CBS overexpression were incubated with NIR-HS ( $5 \mu M$ ) for 10 min (**2A**). Cells transfected with empty vector were incubated with NIR-HS ( $5 \mu M$ ) for 10 min (**2B**). Scale bars =  $10 \mu m$ . The average fluorescence intensity of the above images (**2C**). Data are presented as the mean  $\pm$  SD ( $n = 3$ ). \* $p < 0.001$  vs. (1A) column, ## $p < 0.001$  vs. (2A) column.

A), and the mice were given i.p. injection of free probe as the probe-loaded group (Fig. 6, panels A). One group were pretreated with  $ZnCl_2$ , and then injected with free probe (Supplementary Fig. S13, panel B). The other three groups were injected with different amounts of  $Na_2S$  (1, 5 and 10 equiv.) after i.p. injection of probe (Fig. 6, panels B, C and D). The last group were given i.p. injection of SNP and followed by i.p. injection with the probe. The mice were imaged using a Night OWL IILB 983 small animal *in vivo* imaging system. The fluorescent images showed almost no background fluorescence in the negative control group (Supplementary Fig. S13, panel A; panel C,  $R = 0.12$  in column A), and weak fluorescence in the probe-loaded group (Fig. 6, panel A; panel E,  $R = 1.0$  in column A), which suggests weak fluorescence signals in probe-loaded mice may be caused by endogenous  $H_2S$ . To confirm this assumption, we pretreated (i.p. injection) another group of mice with  $ZnCl_2$  (an efficient eliminator of  $H_2S$ ). After 10 min of  $ZnCl_2$ -treatment, the mice were given i.p. injection of free probe. Compared with the free probe-loaded mice, the fluorescence of  $ZnCl_2$ -treated group is remarkably weakened (Supplementary Fig. S13, panel B,  $R = 0.18$  in column B), indicating that the weak fluorescence in probe-loaded mice is triggered by physiological concentration of endogenous  $H_2S$ . The mice treated with both  $Na_2S$  (1, 5 and 10 equiv.) and the probe displayed much higher fluorescence (Fig. 6, panels B, C and D) than the mice treated with only the probe, which demonstrate that NIR-HS could respond to exogenous sulphide in mice. Moreover, the mice injected with SNP (Sodium Nitroprusside, a NO donor, could induce the production of endogenous  $H_2S$ ) and probe showed a marked elevation in the fluorescence intensities from the abdominal area of the mice (Fig. 6, panel E,  $R = 3.4$  in column E), indicating that NIR-HS was sensitive enough to detect endogenous  $H_2S$  in living mice. Importantly, the fluorescence intensities from the abdominal area of the mice were quantified, and the data showed that the fluorescence intensities triggered by  $Na_2S$  were concentration-dependent ( $R = 1.0$  in column A,  $R = 1.6$  in column B,  $R = 3.5$  in column C,  $R = 4.8$  in column D) (Fig. 6, panel F). Figure 7 demonstrated that the fluorescence intensities became strong gradually within 20 min, consistent with the results of titrating the probe with  $Na_2S$  at different time in PBS buffer (Supplementary Fig. S2). These experiments suggested that NIR-HS is suitable for monitoring exogenous and endogenous  $H_2S$  in living mice.

Recently, the development of fluorescent probes for  $H_2S$  *in vivo* is of high interest. A few fluorescent probes have been successfully discovered for imaging of  $H_2S$  in living animals, such as mice<sup>49–51</sup>, zebrafish<sup>52–55</sup> and *Caenorhabditis elegans*<sup>56,57</sup>, *et al.* In addition to fluorescent probes, luminescent probe and chemiluminescent probe have been applied to determining  $H_2S$  in living mice<sup>58,59</sup>. Despite these progresses, the NIR fluorescence imaging of endogenous  $H_2S$  *in vivo* is still highly desirable. Wallace *et al.* utilized fluorescent probe SF5 to investigate the regulation of leukocyte  $H_2S$  synthesis *in vivo*<sup>44</sup>. However, probe SF5 emitted around 520 nm, the visible-light range limited its application for *in vivo* imaging due to the interference of background autofluorescence. Lu *et al.* prepared a novel bioluminescence probe for detection of endogenous  $H_2S$  in nude mice<sup>45</sup>. Nevertheless, for this

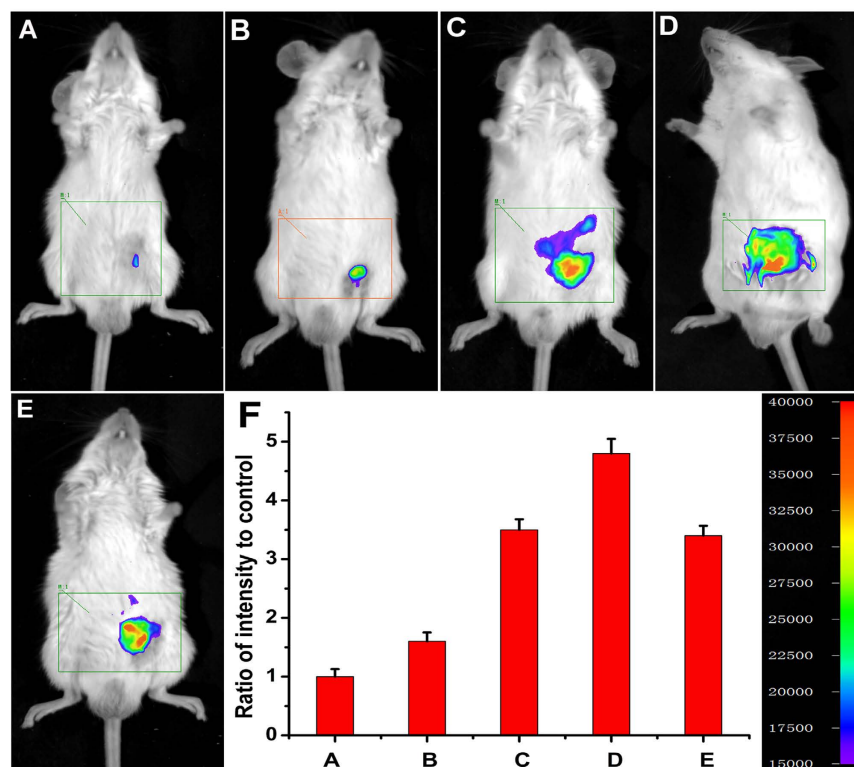


**Figure 6. Representative fluorescence images of visualizing exogenous and endogenous H<sub>2</sub>S in living mice using NIR-HS.** The mice were i.p. injected with the probe NIR-HS (50 μM, in 50 μL DMSO) as the control group (A). The mice were i.p. injected with the probe NIR-HS (50 μM, in 50 μL DMSO), followed by i.p. injection of 1 equiv. Na<sub>2</sub>S (50 μM, in 100 μL saline) (B). The mice were i.p. injected with the probe NIR-HS (50 μM, in 50 μL DMSO), followed by i.p. injection of 5 equiv. Na<sub>2</sub>S (250 μM, in 100 μL saline) (C). The mice were i.p. injected with the probe NIR-HS (50 μM, in 50 μL DMSO), followed by i.p. injection of 10 equiv. Na<sub>2</sub>S (500 μM, in 100 μL saline) (D). The mice were i.p. injected with SNP (200 μM, in 100 μL saline), followed by i.p. injection of NIR-HS (50 μM, in 50 μL DMSO) (E). Quantification of the fluorescence emission intensities from the abdominal area of the mice of the above groups (F). Images were taken after incubation for 20 min. Data are presented as the mean ± SD (*n* = 3).

bioluminescence probe, Cys at 15 μM triggered weak bioluminescence. It is well known that the concentrations of Cys in cells/tissue are much higher compared to the concentrations of endogenous H<sub>2</sub>S, and small response induced by Cys may interfere the detection of H<sub>2</sub>S. Moreover, the H<sub>2</sub>S reaction site of this bioluminescence probe was azide group. The azide-containing H<sub>2</sub>S probes could undergo photoactivation under continuous excitation<sup>60</sup>, rendering them unsuitable for *in vivo* imaging. Thus, NIR probes with high sensitivity, good selectivity and favourable properties to monitor endogenous H<sub>2</sub>S *in vivo* are highly needed. Our probe NIR-HS is more suitable for biological imaging endogenous H<sub>2</sub>S in living mice.

Taken together, we have prepared a novel fluorescent probe NIR-HS for H<sub>2</sub>S detection in living cells and mice. Advantages of this H<sub>2</sub>S-specific probe include emission in the NIR region, a low detection limit, high sensitivity, good selectivity and low cytotoxicity. This probe not only enables fluorescence imaging of endogenous H<sub>2</sub>S induced by SNP in living cells, but also detects endogenous H<sub>2</sub>S generated in cells overexpressing cystathionine β-synthase (CBS). The probe was also successfully applied to visualizing both the exogenous and endogenous H<sub>2</sub>S in living mice. Probe NIR-HS shows the potential to be used as a valuable research tool in studying biological roles of H<sub>2</sub>S. We are currently pursuing other strategies to develop more sensitive and specific fluorescent sensors for monitoring H<sub>2</sub>S in living animals, as well as the H<sub>2</sub>S-related medical studies.

## Methods

**Fluorometric analysis.** All fluorescence measurements were conducted at room temperature on a Hitachi F4600 Fluorescence Spectrophotometer. The probe solution (CH<sub>3</sub>CN) was added to a quartz cuvette. With the probe diluted to 10 μM with 20 mM PBS buffer, Na<sub>2</sub>S was added (Na<sub>2</sub>S·9H<sub>2</sub>O serving as the H<sub>2</sub>S source in all experiments). The resulting solution was then incubated for 20 min. The samples were excited at 670 nm with the excitation and emission slit widths set at 5 nm and 10 nm, respectively. The emission spectrum was scanned from 690 nm to 850 nm at a velocity of 1200 nm/min. The photomultiplier voltage was set at 1000 V. Data are presented as the mean ± SD (*n* = 3).

**Cell culture and confocal fluorescence imaging.** The MCF-7 cells were grown up in DMEM media supplemented with 10% (v/v) FBS (foetal bovine serum) and penicillin/streptomycin (100 μg/mL) at 37 °C in

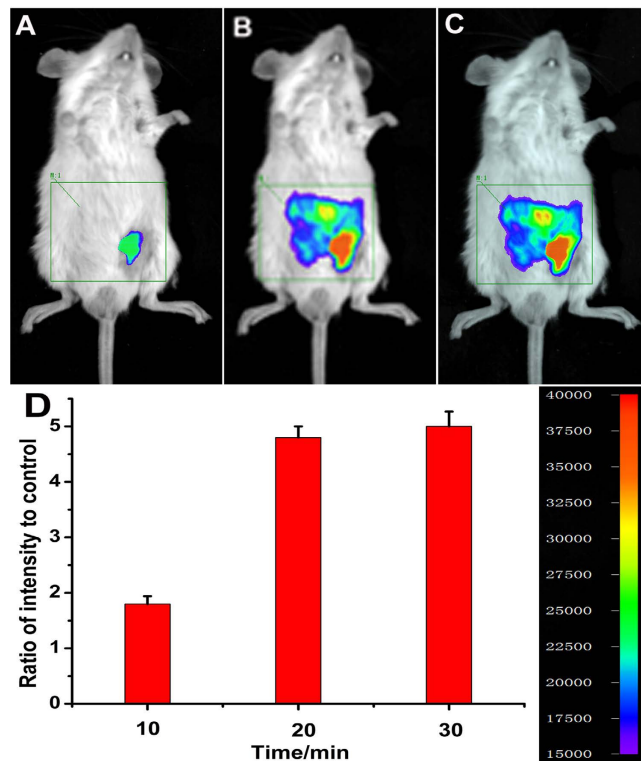


**Figure 7. Representative fluorescence images of visualizing  $H_2S$  levels at different times in living mice using NIR-HS.** The mice were i.p. injected with the probe NIR-HS ( $50 \mu M$ , in  $50 \mu L$  DMSO), followed by i.p. injection of 10 equiv.  $Na_2S$  ( $500 \mu M$ , in  $100 \mu L$  saline). Images were taken after incubation of  $Na_2S$  at: 10 min (A); 20 min (B); 30 min (C). Quantification of the fluorescence emission intensities from the abdominal area of the mice of the above groups (D). Data are presented as the mean  $\pm$  SD ( $n = 3$ ).

a 5%  $CO_2$  incubator. Cells were permitted to grow to 80% confluence before harvesting and transferring to a coverglass (Lab-Tek® II Chambered Coverglass, NalcoNunc, Naperville, USA). A final concentration of  $5 \mu M$  NIR-HS (1.0 mM stock solution in  $CH_3CN$ ) was added to the cell media and incubated at the previous conditions for 10 min. For exogenous sulphide imaging, the cells were thrice rinsed with PBS solution ( $pH = 7.4$ ) to remove excess NIR-HS, which was followed by the addition of  $Na_2S$  (20 mM stock solution in DI  $H_2O$ , final concentration  $25 \mu M$  or  $50 \mu M$ ) for incubation 10 min or 20 min at  $37^\circ C$ . For endogenous sulphide imaging, cells were pretreated with NIR-HS ( $5 \mu M$ ) for 10 min and then stimulated with SNP (sodium nitroprusside, 20 mM stock solution in DI  $H_2O$ , final concentration  $50 \mu M$ ) for 20 min. In addition, cells with CBS overexpression were incubated with NIR-HS ( $5 \mu M$ ) for 10 min. All the cells were thrice rinsed with PBS buffer prior to imaging. Confocal fluorescence imaging was performed on an Olympus FV1000 confocal laser scanning microscope with  $\times 60$  oil objectives. The excitation wavelength was 635 nm. The fluorescence images (660 nm–760 nm) were obtained at  $1024 \times 1024$  pixels, and were analysed with Olympus software (FV10-ASW). All data are expressed as the mean  $\pm$  SD ( $n = 3$ ).

**Animals and administration.** Adult male Kunming mice weighing 20–25 g were provided by the Experimental Animal Centre of Xuzhou Medical College. All of the experiments were performed in compliance with the Chinese legislation on the use and care of laboratory animals and were approved by the Institutional Animal Care and Use of Xuzhou Medical College. The animals were housed in a room with regulated temperature ( $22 \pm 2^\circ C$ ) and humidity ( $50 \pm 10\%$ ) on a 12 h light/dark cycle; the animals had *ad libitum* access to standard commercial animal feed and pure water. Mice were acclimatised for 1 week prior to the experiment.

**Fluorescent imaging in living mice.** The mice were anesthetized by i.p. injection of 10% chloral hydrate ( $0.04 mL/10g$ ), and their abdominal fur was removed. The mice were random selected and divided into several groups. Subsequently, one group were given i.p. injection of DMSO ( $50 \mu L$ ) as the negative control group, and the mice were given i.p. injection of free probe ( $50 \mu M$ , in  $50 \mu L$  DMSO) as the probe-loaded group. One group were pretreated with  $ZnCl_2$  (10 mM, in  $100 \mu L$  saline), and then injected with free probe. The other three groups were i.p. injected with the probe NIR-HS ( $50 \mu M$ , in  $50 \mu L$  DMSO), and followed by i.p. injection with different amount of  $Na_2S$  ( $50 \mu M$ ,  $250 \mu M$  and  $500 \mu M$  in saline). The last group were i.p. injected with SNP ( $200 \mu M$ , in  $100 \mu L$  saline), followed by i.p. injection of NIR-HS ( $50 \mu M$ , in  $50 \mu L$  DMSO). After 20 min, the mice were then imaged by using a Night OWL IILB 983 small animal *in vivo* imaging system, with an excitation filter of 670 nm and an emission filter of 690 nm–740 nm. For the time-dependent experiment, the mice were given i.p. injection

of 10 equiv. Na<sub>2</sub>S (500 μM, in 100 μL saline) after the same disposal of the control mice. Images were then taken at different times (10, 20, and 30 min).

**Western blot.** For western blot analysis, the cells were washed with cold PBS and lysed with RIPA buffer (1% Triton X-100, 1% deoxycholate, 0.1% SDS) containing protease inhibitors (1mM PMSF, 20mM NaF, 1mM NaVO<sub>3</sub>). Protein concentrations were determined using BCA protein assay kits. The cells samples were separated by 10% SDS-polyacrylamide gel electrophoresis (SDS-PAGE) and then transferred onto nitrocellulose membranes (Amersham Pharmacia Biotech). The membranes were blocked with 5% skim milk powder in a washing buffer (Tris-buffered saline containing 0.05% (v/v) Tween 20) for 2 h at 25 °C and subsequently incubated overnight with the primary antibodies specific for CBS (1:1000) and β-actin(1:1000). Each membrane was thrice rinsed for 15 min and incubated with either alkaline phosphatase-conjugated secondary antibodies (1:1000, Goat anti-Rabbit IgG antibody) or alkaline phosphatase-conjugated secondary antibodies (1:1000, Horse anti-Mouse IgG antibody), which was followed by visualization by BCIP/NBT alkaline phosphatase colour development kits. Protein bands were scanned and quantified by densitometric analysis using ImageJ version 1.34 software.

**Construction of CBS overexpressing cells.** The cDNA clones for human CBS were purchased from Origene (lot no.: RC201755). MCF-7 cells were grown to 90% confluence before being transiently transfected with pCMV6-control and pCMV6-CBS expression plasmids using Lipofectamine 2000 (Invitrogen, Shanghai, China) according to the manufacturer's instructions. Six hours after transfection, the medium containing transfection reagents was removed and incubated in fresh medium. The CBS overexpressed cells were harvested for subsequent experiments.

**Statistical analyses.** All statistical analyses were performed using SPSS software, version 16.0 (SPSS Inc., Chicago, IL, USA). Values are expressed as the mean ± SD (standard deviation of the mean). The data were analysed with one-way analysis of variance (ANOVA). Statistical significance was set at  $p < 0.05$ .

## References

- Kabil, O. & Banerjee, R. Redox biochemistry of hydrogen sulphide. *J. Biol. Chem.* **285**, 21903–21907 (2010).
- Kimura, H. Production and physiological effects of hydrogen sulphide. *Antioxid. Redox. Signal.* **20**, 783–793 (2014).
- Kimura, H. Hydrogen sulphide: from brain to gut. *Antioxid. Redox. Signal.* **12**, 1111–1123 (2010).
- Hu, L. F., Lu, M., Hon, Wong, P. T. & Bian, J. S. Hydrogen sulphide: neurophysiology and neuropathology. *Antioxid. Redox. Signal.* **15**, 405–419 (2011).
- Lefer, D. J. A new gaseous signaling molecule emerges: cardioprotective role of hydrogen sulphide. *Proc. Natl. Acad. Sci. USA* **104**, 17907–17908 (2007).
- Yang, G., Wu, L. & Wang, R. Pro-apoptotic effect of endogenous H<sub>2</sub>S on human aorta smooth muscle cells. *FASEB J.* **20**, 553–555 (2006).
- Zanardo, R. C. *et al.* Hydrogen sulphide is an endogenous modulator of leukocyte-mediated inflammation. *FASEB J.* **20**, 2118–2120 (2006).
- Elrod, J. W. *et al.* Hydrogen sulphide attenuates myocardial ischemia-reperfusion injury by preservation of mitochondrial function. *Proc. Natl. Acad. Sci. USA* **104**, 15560–15565 (2007).
- Kaneko, Y., Kimura, Y., Kimura, H. & Niki, I. L-cysteine inhibits insulin release from the pancreatic beta-cell: possible involvement of metabolic production of hydrogen sulphide, a novel gasotransmitter. *Diabetes.* **55**, 1391–1397 (2006).
- Gong, Q. H. *et al.* A new hope for neurodegeneration: possible role of hydrogen sulphide. *J. Alzheimers. Dis.* **24** Suppl 2, 173–182 (2011).
- Szabo, C. Roles of hydrogen sulphide in the pathogenesis of diabetes mellitus and its complications. *Antioxid. Redox. Signal.* **17**, 68–80 (2012).
- Nagy, P. *et al.* Chemical aspects of hydrogen sulphide measurements in physiological samples. *Biochim. Biophys. Acta.* **1840**, 876–891 (2014).
- Yan, Y. Y. *et al.* The small molecule fluorescent probes for gasotransmitters. *Scientia Sinica Chimica.* **45**, 812–828 (2015).
- Qian, Y. *et al.* Selective fluorescent probes for live-cell monitoring of sulphide. *Nat. Commun.* **2**, 495–502 (2011).
- Liu, C. R. *et al.* Capture and visualization of hydrogen sulphide by a fluorescent probe. *Angew. Chem., Int. Ed.* **50**, 10327–10329 (2011).
- Xu, Z. *et al.* A highly selective fluorescent probe for fast detection of hydrogen sulphide in aqueous solution and living cells. *Chem. Commun.* **48**, 10871–10873 (2012).
- Qian, Y. *et al.* A Fluorescent Probe for rapid detection of hydrogen sulphide in blood plasma and brain tissues in mice. *Chem. Sci.* **3**, 2920–2923 (2012).
- Zhang, L. L., Zhu, H. K., Li, M. M. & Gu, X. F. A novel fluorescent probe for imaging endogenous hydrogen sulphide via the CSE enzymatic pathway. *Chem. Commun.* **51**, 13135–13137 (2015).
- Zhang, J., Sun, Y. Q., Liu, J., Shi, Y. & Guo, W. A fluorescent probe for the biological signaling molecule H<sub>2</sub>S based on a specific H<sub>2</sub>S trap group. *Chem. Commun.* **49**, 11305–11307 (2013).
- Gu, X. F., Zhu, H. K., Yang, S., Zhu, Y. C. & Zhu, Y. Z. Development of a highly selective H<sub>2</sub>S fluorescent probe and its application to evaluate CSE inhibitors. *RSC. Adv.* **4**, 50097–50101 (2014).
- Cao, X., Lin, W. & He, L. A near-infrared fluorescence turn-on sensor for sulphide anions. *Org. Lett.* **13**, 4716–4719 (2011).
- Sasakura, K. *et al.* Development of a highly selective fluorescence probe for hydrogen sulphide. *J. Am. Chem. Soc.* **133**, 18003–18005 (2011).
- Li, X. *et al.* A highly specific probe for sensing hydrogen sulphide in live cells based on copper-initiated fluorogen with aggregation-induced emission characteristics. *Theranostics.* **4**, 1233–1238 (2014).
- Lippert, A. R., New, E. J. & Chang, C. J. Reaction-based fluorescent probes for selective imaging of hydrogen sulphide in living cells. *J. Am. Chem. Soc.* **133**, 10078–10080 (2011).
- Peng, H. *et al.* A fluorescent probe for fast and quantitative detection of hydrogen sulphide in blood. *Angew. Chem. Int. Ed. Engl.* **50**, 9672–9675 (2011).
- Lin, V. S., Lippert, A. R. & Chang, C. J. Cell-trappable fluorescent probes for endogenous hydrogen sulphide signaling and imaging H<sub>2</sub>O<sub>2</sub>-dependent H<sub>2</sub>S production. *Proc. Natl. Acad. Sci. USA* **110**, 7131–7135 (2013).
- Bae, S. K. *et al.* A ratiometric two-photon fluorescent probe reveals reduction in mitochondrial H<sub>2</sub>S production in Parkinson's disease gene knockout astrocytes. *J. Am. Chem. Soc.* **135**, 9915–9923 (2013).



28. Zhang, L. *et al.* A colorimetric and ratiometric fluorescent probe for the imaging of endogenous hydrogen sulphide in living cells and sulphide determination in mouse hippocampus. *Org. Biomol. Chem.* **12**, 5115–5125 (2014).
29. Zhang, L. *et al.* Selective detection of endogenous H<sub>2</sub>S in living cells and the mouse hippocampus using a ratiometric fluorescent probe. *Sci. Rep.* **4**, 5870–5879 (2014).
30. Liu, T., Xu, Z., Spring, D. R. & Cui, J. A lysosome-targetable fluorescent probe for imaging hydrogen sulphide in living cells. *Org. Lett.* **15**, 2310–2313 (2013).
31. Cao, X., Lin, W., Zheng, K. & He, L. A near-infrared fluorescent turn-on probe for fluorescence imaging of hydrogen sulphide in living cells based on thiolysis of dinitrophenyl ether. *Chem. Commun.* **48**, 10529–10531 (2012).
32. Zhao, C. C. *et al.* Förster resonance energy transfer switchable self-assembled micellar nanoprobe: ratiometric fluorescent trapping of endogenous H<sub>2</sub>S generation via fluvastatin-stimulated upregulation. *J. Am. Chem. Soc.* **137**, 8490–8498 (2015).
33. Nolting, D. D., Gore, J. C. & Pham, W. Near-Infrared dyes: probe development and applications in optical molecular imaging. *Curr. Org. Synth.* **8**, 521–534 (2011).
34. Yuan, L., Lin, W., Zheng, K., He, L. & Huang, W. Far-red to near infrared analyte-responsive fluorescent probes based on organic fluorophore platforms for fluorescence imaging. *Chem. Soc. Rev.* **42**, 622–661 (2013).
35. Yu, F. *et al.* An ICT-based strategy to a colorimetric and ratiometric fluorescence probe for hydrogen sulphide in living cells. *Chem. Commun.* **48**, 2852–2854 (2012).
36. Ozdemir, T., Sozmen, F., Mamur, S., Tekinay, T. & Akkaya, E. U. Fast responding and selective near-IR Bodipy dye for hydrogen sulphide sensing. *Chem. Commun.* **50**, 5455–5457 (2014).
37. Wang, R. *et al.* A highly selective turn-on near-infrared fluorescent probe for hydrogen sulphide detection and imaging in living cells. *Chem. Commun.* **48**, 11757–11759 (2012).
38. Cao, X., Lin, W., Zheng, K. & He, L. A near-infrared fluorescent turn-on probe for fluorescence imaging of hydrogen sulphide in living cells based on thiolysis of dinitrophenyl ether. *Chem. Commun.* **48**, 10529–10531 (2012).
39. Chen, Y. *et al.* A ratiometric fluorescent probe for rapid detection of hydrogen sulphide in mitochondria. *Angew. Chem., Int. Ed.* **52**, 1688–1691 (2013).
40. Wang, X. *et al.* A near-infrared ratiometric fluorescent probe for rapid and highly sensitive imaging of endogenous hydrogen sulphide in living cells. *Chem. Sci.* **4**, 2551–2556 (2013).
41. Qu, X. *et al.* A red fluorescent turn-on probe for hydrogen sulphide and its application in living cells. *Chem. Commun.* **49**, 7510–7512 (2013).
42. Sun, W. *et al.* A two-photon fluorescent probe with near-infrared emission for hydrogen sulphide imaging in biosystems. *Chem. Commun.* **49**, 3890–3892 (2013).
43. Chen, H., Lin, W., Cui, H. & Jiang, W. Development of unique xanthene-cyanine fused near-infrared fluorescent fluorophores with superior chemical stability for biological fluorescence imaging. *Chemistry*. **21**, 733–745 (2015).
44. Dufton, N., Natividad, J., Verdu, E. F. & Wallace, J. L. Hydrogen sulfide and resolution of acute inflammation: A comparative study utilizing a novel fluorescent probe. *Sci. Rep.* **2**, 499–509 (2012).
45. Tian, X., Li, Z., Lau, C. & Lu, J. Visualization of *in Vivo* Hydrogen Sulfide Production by a Bioluminescence Probe in Cancer Cells and Nude Mice. *Anal. Chem.*, doi: 10.1021/acs.analchem.5b03712. (2015).
46. Yuan, L. *et al.* A unique approach to development of near-infrared fluorescent sensors for *in Vivo* imaging. *J. Am. Chem. Soc.* **134**, 13510–13523 (2012).
47. Lv, M., Li, Y., Ji, M. H., Zhuang, M. & Tang, J. H. Inhibition of invasion and epithelial-mesenchymal transition of human breast cancer cells by hydrogen sulfide through decreased phospho-p38 expression. *Mol. Med. Rep.* **10**, 341–346 (2014).
48. Zhao, W., Zhang, J., Lu, Y. & Wang, R. The vasorelaxant effect of H<sub>2</sub>S as a novel endogenous gaseous K(ATP) channel opener. *EMBO J.* **20**, 6008–6016 (2001).
49. Sun, W. *et al.* A two-photon fluorescent probe with near-infrared emission for hydrogen sulfide imaging in biosystems. *Chem. Commun.* **49**, 3890–3892 (2013).
50. Chen, H., Lin, W., Cui, H. & Jiang, W. Development of unique xanthene-cyanine fused near-infrared fluorescent fluorophores with superior chemical stability for biological fluorescence imaging. *Chemistry*. **21**, 733–745 (2015).
51. Wu, H. *et al.* Highly selective and sensitive near-infrared-fluorescent probes for the detection of cellular hydrogen sulfide and the imaging of H<sub>2</sub>S in mice. *Chem. Asian. J.* **9**, 3604–3611 (2014).
52. Hammers, M. D. *et al.* A bright fluorescent probe for H<sub>2</sub>S enables analyte-responsive, 3D imaging in live zebrafish using light sheet fluorescence microscopy. *J. Am. Chem. Soc.* **137**, 10216–10223 (2015).
53. Wan, Q., Song, Y., Li, Z., Gao, X. & Ma, H. *In vivo* monitoring of hydrogen sulfide using a cresyl violet-based ratiometric fluorescence probe. *Chem. Commun.* **49**, 502–504 (2013).
54. Sathyadevi, P., Chen, Y. J., Wu, S. C., Chen, Y. H. & Wang, Y. M. Reaction-based epoxide fluorescent probe for *in vivo* visualization of hydrogen sulfide. *Biosens. Bioelectron.* **68**, 681–687 (2015).
55. Liu, T. *et al.* Imaging of living cells and zebrafish *in vivo* using a ratiometric fluorescent probe for hydrogen sulfide. *Analyst.* **140**, 7165–7169 (2015).
56. Zhang, W., Kang, J., Li, P., Wang, H. & Tang, B. Dual signaling molecule sensor for rapid detection of hydrogen sulfide based on modified tetraphenylethylene. *Anal. Chem.* **87**, 8964–8969 (2015).
57. Zou, X. J. *et al.* A lysosome-targeted fluorescent chemodosimeter for monitoring endogenous and exogenous hydrogen sulfide by *in vivo* imaging. *Chem. Commun.* **50**, 13833–13836 (2014).
58. Cao, J. *et al.* Chemiluminescent Probes for Imaging H<sub>2</sub>S in Living Animals. *Chem. Sci.* **6**, 1979–1985 (2015).
59. Liu, F., Gao, Y., Wang, J. & Sun, S. Reversible and selective luminescent determination of ClO<sup>-</sup>/H<sub>2</sub>S redox cycle *in vitro* and *in vivo* based on a ruthenium trisbipyridyl probe. *Analyst.* **139**, 3324–3329 (2014).
60. Bailey, T. S. & Pluth, M. D. Chemiluminescent detection of enzymatically produced hydrogen sulfide: substrate hydrogen bonding influences selectivity for H<sub>2</sub>S over biological thiols. *J. Am. Chem. Soc.* **135**, 16697–16704 (2013).

## Acknowledgements

This project was financed by the National Natural Science Foundation of China (21502163 to L. Z.), the Jiangsu Natural Science Foundation (BK20150206 to L. Z.), the Post-doctoral Fund in Jiangsu Province (1501034B to L. Z.), the Natural Science Foundation for Colleges and Universities in Jiangsu Province (14KJB350005 to L. Z.), and the Laboratory of Encephalopathy and Bioinformation of Jiangsu Province (Jsbl1204 to L. Z.). The authors also acknowledge support for this work by the Priority Academic Programme Development of Jiangsu Higher Education Institutions.

## Author Contributions

J.Z., L.Z. and Y.L. conceived the idea and directed the work. L.Z. designed the experiments. L.Z., Y.S. and W.M. performed the synthesis. L.Z., F.Z. X.Z. and Z.X. performed the cell-based imaging. L.Z. and E.L. performed the

*in vitro* fluorescence tests L.Z. and X.Z. performed the *in vivo* imaging. All authors contributed to the data analysis and to writing the manuscript.

### Additional Information

**Supplementary information** accompanies this paper at <http://www.nature.com/srep>

**Competing financial interests:** The authors declare no competing financial interests.

**How to cite this article:** Zhang, L. *et al.* A highly selective and sensitive near-infrared fluorescent probe for imaging of hydrogen sulphide in living cells and mice. *Sci. Rep.* **6**, 18868; doi: 10.1038/srep18868 (2016).



This work is licensed under a Creative Commons Attribution 4.0 International License. The images or other third party material in this article are included in the article's Creative Commons license, unless indicated otherwise in the credit line; if the material is not included under the Creative Commons license, users will need to obtain permission from the license holder to reproduce the material. To view a copy of this license, visit <http://creativecommons.org/licenses/by/4.0/>